

Low Cost and Simple P&O-MPP Tracker Using Flyback Converter

Salam J. Yaqoob¹, Ahmed Raisan Hussein², Ameer L. Saleh³

¹Popular Mobilization, Prime Minister Office, Baghdad, Iraq,

^{2,3}Department of Electrical Engineering, College of Engineering, Misan University, Misan, Iraq

ameer-lateef@uomisan.edu.iq

Abstract: In this paper, a low cost and simple MPP tracker using flyback converter are proposed. First, MPP tracker is defined by a theoretical analysis approach of the relationship between the equivalent resistance, load resistance and duty cycle of the flyback converter. Secondly, based on this way the perturbation of the Photovoltaic (PV) power is determined and then the duty cycle of the flyback converter is adjusting to achieve the maximum power point (MPP) correctly. If the alteration in the power is less than zero, the duty cycle is incremented. On the other hand, the duty cycle is decremented if the alteration in the power is greater than zero until to reach the optimal working point. To verify the performance of this proposed MPP tracker, a PSIM software is utilized to investigate the results of the proposed technique with rapid change in both cell ambient temperature and solar irradiance. In addition, the sample algorithm is written directly using simple C-block code without the need the analogue devices that built the conventional MPP tracker. As present in simulation results, exhibit a fast response in high irradiance level is achieved with small oscillation value. Finally, the oscillation problem around the MPP is avoided using a small perturbation step.

Keywords: low cost MPP tracker, simple MPP tracker, maximum power point tracking(MPPT), flyback converter.

1 Introduction

The Photovoltaic system is the most known of solar energy kinds. Solar energy is exploited by utilizing solar electric systems; the word photovoltaic is originated from the photo (light) and voltaic (voltage). The PV cell straightway converts the sunlight into electrical energy by the PV effect. Since a standard PV cell produces about 1 or 2 W of power. The PV cells are configured into arrays, and then the arrays are connected as panels to boost the output power of the PV cells. Where the output power of the PV system depends on the atmosphere factors such as solar irradiation and the temperature.

For this reason, any increase in the temperature of the PV system, the voltage of the PV system decreases, while the current increases slightly [1-3]. The resultant influence decreases the power of the PV system. On other hand, when the solar irradiation is increased, the PV system current is more increased; which is proportional straightway to the solar irradiation, while the voltage of the PV system exposes little variation [4,5]. On the other hand, the voltage of the PV cell is between 0.5 V to 0.7 V while the cell current is about 30 mA/cm². For this reason, PV cells are connected in series to form a panel and boost the overall PV voltage. The PV cell is a time-variant power generator. This problem can be caused by solar radiation and

variation in cell temperature. Therefore, the MPP of the PV module is always changing. For this reason, the MPPT technique is utilized to track the MPP of the power at different weather condition. Today, an assortment of MPPT techniques have been suggested and reviewed continuously [6,7]. Mainly, the choice of an MPPT technique is depended on many limitations such as cost, response speed, complexity, oscillation around the MPP, sensors. These techniques such as perturb and observe (P&O) [8,9], incremental conductance(IC) [10,11], fractional open-circuit voltage, fractional short-circuit current [12], Hill Climbing (HC) [13], fuzzy logic system, neural network, adaptive fuzzy-neural [14-17]. A P&O technique is vastly utilized due to its simplicity, low computation processes. In this technique, the PV voltage is perturbed by a small step value and the variation of the power is observed. This process continues in the same trend until the increment in power is stopped. If the changing in PV power is less than zero, the operating point will move far from the MPP, and then the trend of perturbation is inverted to returning toward the MPP. In this paper, a low cost and simple MPP tracker is proposed based on perturbation only of PV power and observed the duty cycle of the flyback converter. Power simulator software (PSIM) is considered as one of the major toolboxes for modelling, analyzing, solving dynamic system and real problems; therefore, it will be utilized for modelling and simulation the proposed overall PV system. Thus, the proposed algorithm code is written in simple C-block of PSIM software without the need of the analog model of P&O technique.

2 Photovoltaic Cell Model

The equivalent circuit that is depicts in Fig. 1, represents a PV cell model. This model is also known as a one-diode model [18]. It is based on a supposition that the re-composition loss in the depletion region is negligible. One-diode model is widely utilized for the most PV applications due to its suitability and simplicity. Hence, from the principle of semiconductors, the basic equation which represents the I–V characteristic of the ideal PV cell the output current I_{PV} can be expressed as [19].

$$I_{PV} = I_{PH} - I_0 \left[\exp\left(\frac{q V_{PV}}{\alpha K T}\right) - 1 \right] \quad (1)$$

V_{PV} is "the output voltage of PV cell", I_{PH} is "the source of photo-current", I_0 is the diode saturation current of PV cell, α is the diode ideality constant ($\alpha = 1.3$) and q is "the charge of electron ($1.60217646 \times 10^{-19}C$)". K is "the Boltzmann constant, ($1.3806503 \times 10^{-23} J/^{\circ}K$)" and the temperature of the p-n junction in $^{\circ}K$ is "represented by T ". The series and parallel resistances should be taken in account of the equivalent circuit of PV cell to observe a real PV cell. Therefore, the output current re-written as [19]:

$$I_{PV} = I_{PH} - I_0 \left[\exp\left(\frac{q V_{PV}}{\alpha V_T}\right) - 1 \right] - \frac{V_{PV} + R_S I_{PV}}{R_P} \quad (2)$$

where $V_T (= N_S K T / q)$ is the thermal voltage (25.7mV at 25 $^{\circ}C$) with N_S number of cells connected in series. R_P and R_S are the parallel and series resistances, respectively.

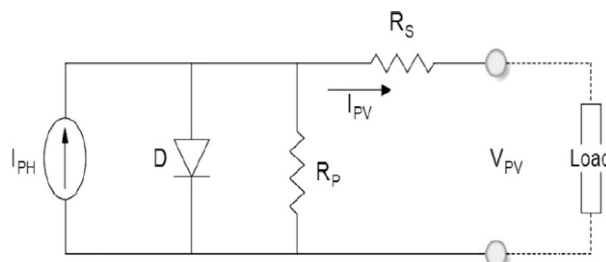


Fig. 1. Equivalent circuit of one-diode PV cell model.

All PV panels are provided by datasheet that include standard test condition parameters as open-circuit voltage (V_{oc}), short circuit current (I_{sc}), the voltage at MPP (V_{mp}), the current at MPP (I_{mp}), the temperature coefficient for the case of open circuit voltage (K_v), the temperature coefficient for case short circuit current (K_i) and experimental maximum power (P_{mp}). These parameters are always given with indicate to typical test situation of temperature and solar irradiance. On the other hand, a series resistance (R_s) and a parallel (R_p) are not provided in the datasheet, it can be evaluated independently [20]. However, I_{PH} depends linearly on the solar irradiance that falling on the surface of the PV panel and its influenced by the ambient temperature of PV panel as depicts below [20].

$$I_{PH} = (I_{PHn} + K_i \Delta T) \frac{G}{G_n} \tag{3}$$

where I_{PHn} is "the photo-current at Standard Test Conditions (STC)", $\Delta T = T - T_n$ ($T_n = 25^\circ C$), G is the fallen of irradiation on the panel and G_n ($1000W/m^2$) at STC. K_i is "the coefficient for temperature at case short circuit current". In addition, the diode saturation current equation can be expressed as [21]:

$$I_0 = I_{0n} \left(\frac{T_n}{T}\right)^3 \exp\left[\frac{qE_g}{\alpha K} \left(\frac{1}{T_n} - \frac{1}{T}\right)\right] \tag{4}$$

I_{0n} is the reverse saturation current of diode at STC and E_g is the band gap energy ($E_g = 1.12ev$). Table 1 shows the electrical parameters of PV panel that used in this work.

Table 1
Electrical quantities of the PV panel under STC condition.

Quantity	Value	Unit
V_{mpp}	17.1	V
I_{mpp}	3.5	A
P_{mpp}	60	W
V_o	21.1	V
I_{sc}	3.8	A
K_i	0.065	percent/ $^\circ C$
K_v	-0.38	mV/ $^\circ C$
N_s	36	-

3 Flyback Converter Analysis

Mostly, DC/DC converters are utilized to elicit the maximum output power from a PV panel for the purpose of MPPT technique [22-24]. A flyback converter is widely utilized as one type of DC/DC converters in low power applications. This converter has more advantages over other topologies with higher efficiency [25]. Figure 2 shows the flyback configuration circuit which used to acquire maximum output power from a PV panel. It represented an isolated DC/DC converter with higher frequency (HF) transformer, single MOSFET in the primary side, and a diode with output capacitor on the secondary side. The flyback converter is operated in both modes, continuous conduction mode(CCM) and discontinuous conduction mode(DCM). When the flyback converter operated in CCM with continuous magnetizing current, as indicates in Fig.3, the peak primary current is lower than that when the flyback is operating in DCM, so that converter turn OFF losses is lower as well and hence higher efficiency. The energy that transferred to output based on two states of the operation as follows:

ON state: When the main MOSFET, S_{pv} is turned ON as presented in Fig4-a, the DC input voltage of PV panel is impressed across the primary winding of the transformer, which causes stored energy in magnetizing inductance of the transformer and then the primary current slope up to reach its peak value. At the same time, the diode D_o is turned OFF. Thus, the energy stored in magnetizing inductance at ON time interval only. In addition, the HF transformer has a magnetizing inductance, which guarantees not only isolation but also voltage conversion.

OFF state: Here the main MOSFET S_{pv} is turned OFF, and the output diode, D_o is turned ON as show Fig.4-b. Therefore, the energy stored is delivered to the output side.

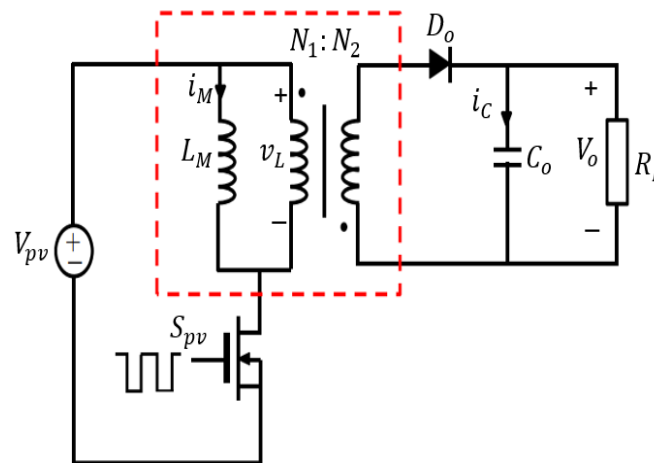


Fig. 2. Flyback converter circuit.

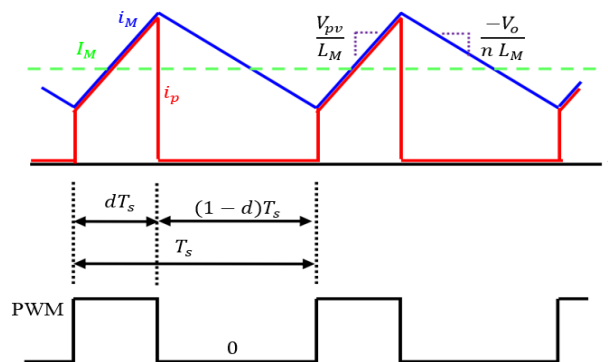


Fig. 3. Waveforms of magnetizing current, I_M primary MOSFET current, I_p and the PWM signals.

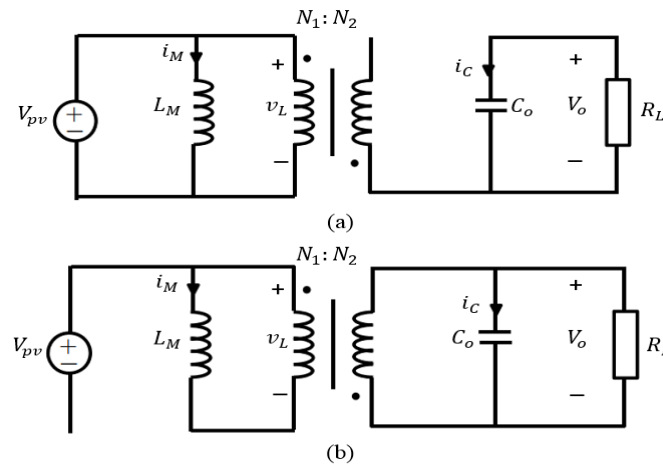


Fig.4. Flyback converter circuit: (a) during time interval one (b) during time interval second

Furthermore, with the supposition that the flyback converter operates with small ripple in the inductor current and small ripple in the capacitor voltage, then the inductor voltage, v_L and capacitor current, i_C are expressed as:

$$v_L = V_{pv} \quad (5)$$

$$i_C = -\frac{V_o}{R_L} \quad (6)$$

where V_{pv} is the PV panel voltage, V_o is the flyback output voltage, R_L is the load resistance. Then, the MOSFET, S_{pv} is turned OFF during time interval second ($dT_s < t < (1-d)T_s$) when the PWM signal is low and the diode conducts. For this reason, the inductor voltage and capacitor current in this interval can be written as [26,27]:

$$v_L = \frac{V_o}{n} \quad (7)$$

where n is the transformer turns-ratio ($n = \frac{N_1}{N_2} = 10$).

$$i_C = \frac{i_{LM}}{n} - \frac{V_o}{R_L} \quad (8)$$

where I_M is the dc component of magnetizing current. Furthermore, the fundamentals of volt-second balance situation and charge balance are utilized to the magnetizing inductance and the output capacitor, respectively [26].

$$\langle v_L \rangle = \frac{1}{T_s} \int_0^{T_s} v_L(t) dt = d(V_{pv}) + (1-d) \left(-\frac{V_o}{n} \right) = 0 \quad (9)$$

Where T_s is the total switching period and d is the duty cycle.

$$\langle i_C \rangle = \frac{1}{T_s} \int_0^{T_s} i_C(t) dt = d \left(-\frac{V_o}{R_L} \right) + (1-d) \left(\frac{I_M}{n} - \frac{V_o}{R_L} \right) = 0 \quad (10)$$

From equation (5), the relationship between the input voltage and output voltage can be expressed as [25]:

$$V_o = V_{pv} \frac{d}{1-d} n \quad (11)$$

Equation (6) produces the dc component value of the magnetizing current as function of duty cycle, d and turns ratio, n as follows:

$$i_{LM} = \frac{n V_o}{(1 - d) R_L} \quad (12)$$

The magnetizing current increases linearly during the time interval one with slope of $\frac{V_{pv}}{L_M}$. In addition, this current decrease during the time interval second with a slope of $\left(\frac{-V_o}{n L_M}\right)$, then this current drops to the same starting point at the end of the switching period. On the other hand, during the MOSFET, S_{pv} is ON, the dc input voltage across the primary winding is the same PV panel voltage, then the primary current, I_p can be expressed as follows:

$$i_p = \frac{V_{pv} d T_s}{L_M} \quad (13)$$

However, in the flyback converter the voltage conversion provide a wide range for input voltage, which is represented a desired condition for MPPT operation [25]. The input resistance R_{in} or the resistance, which is seen by the PV panel, can be expressed by:

$$R_{in} = R_L n^2 \frac{(1 - d)^2}{d^2} \quad (14)$$

Table 2 shows the simulation parameters of flyback converter that used in this work.

Table 2

Simulation parameters of flyback converter circuit.

Parameter	Value	Unit
Output voltage V_o	60	V
Output current I_o	0.98	A
Max. Duty cycle D	0.8	-
Load resistance R	60	Ω
Switching frequency f_s	20	kHz
Magnetizing inductance L_M	10	μH
Output capacitor C	470	μF
Transformer turns ratio n	10	-

4 The Proposed MPP Tracker

The matching between a PV panel and the resistive load is necessary to raise the size of the PV panel requirements to ensure the supply of the power range of the load. This lead to raise the overall PV system cost. For this reason, to solve this problem and improve the performance of the PV panel, an MPPT algorithm is utilized to remain the operating point of the PV panel at MPP. The MPPT is utilized to adjusted the duty cycle ratio of the flyback converter. Where the load resistance seen by the source (matching between the input resistance and the load resistance) is controlled by the duty cycle. Thus, by varying the duty cycle ratio for constant turns-ratio, the input resistance, R_{in} can coincide with the optimal resistance at which the maximum power will be performed from the PV panel. Thus, from equation (10), the input resistance depends on the load resistance

and duty cycle for constant turns-ratio($n=10$), thus the operating point is setting by the intersection of the I-V load characteristic of the PV panel with the load line. When the load line intersects with the I-V curve at point MPP the maximum power is delivered to the load present in Fig.5.

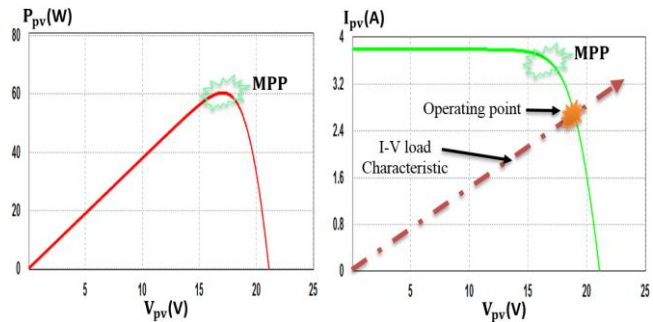


Fig. 5. P-V and I-V panel characteristics under STC condition.

Furthermore, several criteria to select appropriate MPPT technique according to cost, sensors required response time or convergence speed, and complexity. So, a low cost and simple perturb and observe (P & O) algorithm is proposed in this paper. Figure 6 depicts the P-V characteristic of PV panel with proposed MPP tracker. Depends on the variation in the PV power, the MPP is tracked correctly. If the variation in PV power is positive (in left side) for P-V characteristic, ($P_{pv}(k) - P_{pv}(k-1) > 0$), the PV power is increased until it reach to zero change ($P_{pv}(k) - P_{pv}(k-1) = 0$), then the MPP is achieved. On other hand, if the change is negative (in right side) for P-V characteristic, the PV power is decreased until it reach to zero change ($P_{pv}(k) - P_{pv}(k-1) = 0$), then the MPP is achieved. Depending on the flowchart of proposed MPP tracker that presented in Fig.7, by adjusting the duty cycle of the flyback converter, the MPP is accomplished correctly. If the variation in power is less than zero, the duty cycle is incremented. On the other hand, the duty cycle is decremented if the variation in power is greater than zero. When MPP has been achieved, the operation of the PV panel is retained at this point and the perturbation stopped unless a variation in PV power is observed. In this situation, the algorithm increments or decrements the duty cycle to track the new MPP. In addition, the perturbation step size determines how fast the MPP is tracked. In this work, the perturbation step size is chosen carefully (increment=0.01).

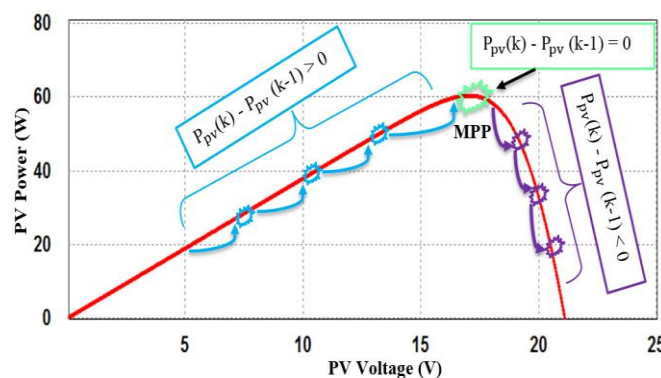


Fig. 6. P-V characteristic of PV power in proposed MPP tracker.

5 Simulation Results and Discussion

The proposed MPP tracker simulation results are carried out using power simulation software (PSIM). Figure 8 shows the proposed system components PV panel model, proposed MPP tracker, and flyback

converter in PSIM. Firstly, the proposed MPP tracker is tested under constant weather condition of solar irradiance, $G = 1000\text{W/m}^2$ and ambient temperature, $T = 25\text{C}^\circ$. Figure 9 depicts the input and output voltage for the flyback converter under constant load condition ($R = 60\Omega$). The input voltage represents the output voltage of the PV panel, that is raised by flyback converter based on turns-ratio and duty cycle. As present, small ripple in output voltage is occurred due to the ripple problem in PV voltage therefore, a capacitor with capacitance of $C_{in} = 1000\mu\text{F}$ is putted in input side of converter as decoupling device.

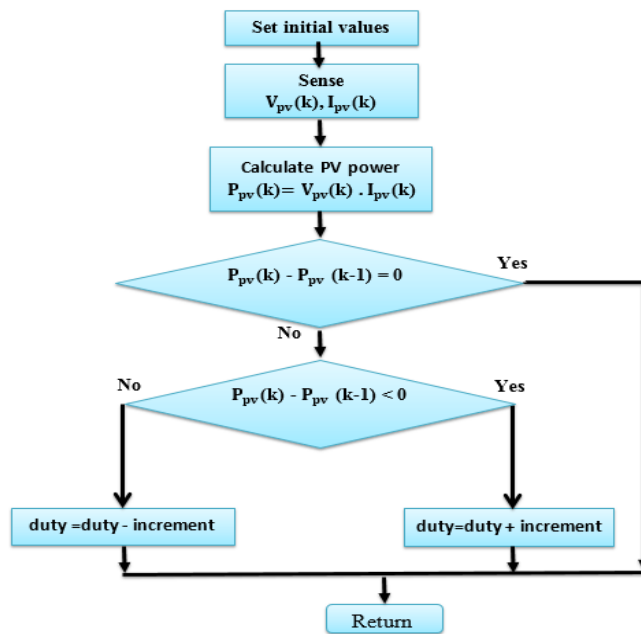


Fig. 7. the flowchart of proposed MPP tracker.

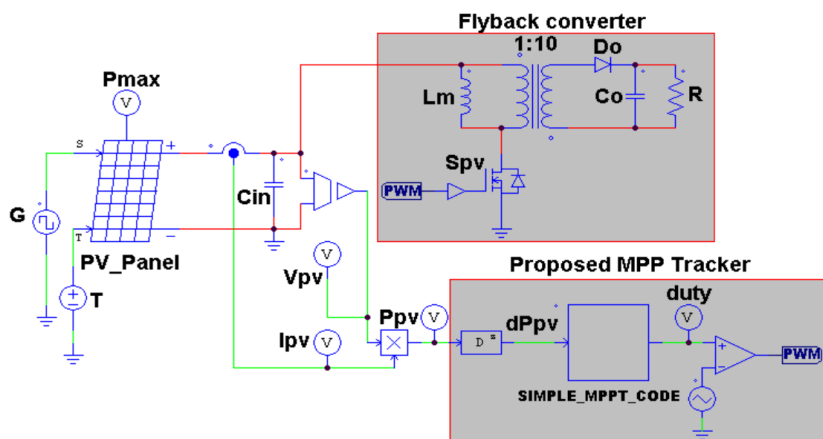


Fig. 8. PV system components in PSIM.

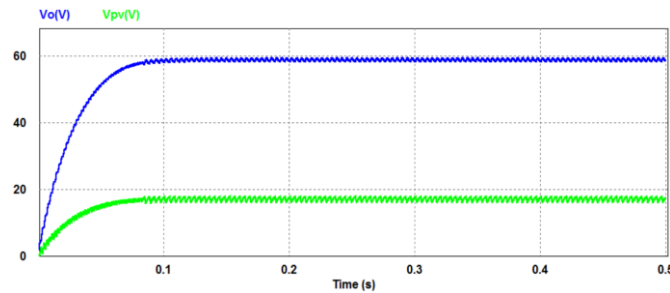


Fig. 9. Input and output voltage for flyback converter.

The flyback simulation results are shown in Fig.10 included PWM signal, Drain-Source voltage, and primary current.

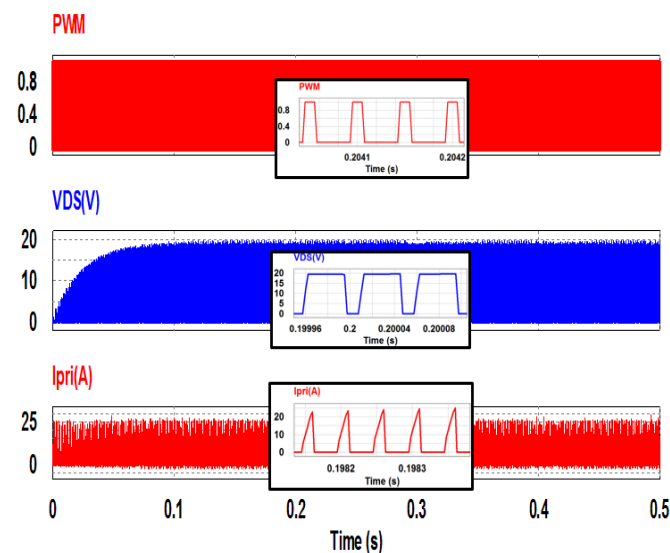


Fig. 10. Simulation results of flyback converter at constant weather condition. Top to bottom: PWM signal, Drain-Source voltage, primary current.

As result, the Drain-Source voltage of the MOSFET is limited to suitable value (20V) without spike voltage problem. Secondly, the system performance is assessed under rapid change of irradiance and constant temperature $T = 25C^{\circ}$ as indicated in Fig.11. When the solar irradiance is changed rapidly from $G = 1000W/m^2$ to $G = 500W/m^2$, the output voltage is decreased to half from $V_o = 60V$ to $V_o = 30V$ and output current also is decreased from $I_o = 0.98A$ to $I_o = 0.48A$. Thus, the output current and voltage of flyback converter are proportionally to the solar irradiance level, so that high output power is elicited from the PV panel at higher irradiance level. However, the solar irradiance is daily changed (not constant) for this reason, the PV power is changed continuously during all day. In order to acquire maximum power from this panel, MPP tracker is utilized to tracking the MPP of the PV panel at any weather condition and result increasing of PV panel efficiency.

The performance of the proposed MPP tracker is tested under both rapid change irradiance and rapid change temperature. Figure 12 shows the simulation results of PV power that tracked by proposed method according to ideal PV power (maximum power). As present, the proposed tracker is succeed correctly by getting the MPP from the PV panel under change of irradiance with small ripple resolution. The proposed tracker exhibit a fast response in high irradiance level depending on the proposed simple algorithm and acceptable response in low irradiance level but a large oscillation occurred after steady state condition.

Hence, oscillation problem in proposed tracker is avoided using small perturbation step size. In addition, the proposed algorithm is utilized to control the duty cycle of MOSFET based on the variance in the PV power as presented in Fig.13, where the increment or decrement in duty cycle depends on the power calculation. Thus, when the solar irradiance is changed rapidly, the proposed algorithm calculated the PV power, sense the difference, and then it can changed duty cycle correctly. Furthermore, the proposed tracker is tested with rapid change in temperature as presented in Fig.14, where the temperature is reduced from $T = 25^{\circ}\text{C}$ to $T = -2^{\circ}\text{C}$ at constant irradiance $G = 1000\text{W}/\text{m}^2$. As result, the output current and voltage of flyback converter are not large sensitive to the change of temperature comparison to the change in irradiance level. This fact due to the mathematical equation for the terminal PV voltage and photo-current source. In addition, small increasing in PV power occurred due to the reduction in cell temperature. Figure 15 shows the tracking of PV power for proposed MPP tracker according to ideal PV power. A fast dynamic response for this change is obtained using proposed method, with small ripple and high power value. The duty cycle is corrected by calculation of the changing in PV power based on proposed algorithm as present in Fig.16.

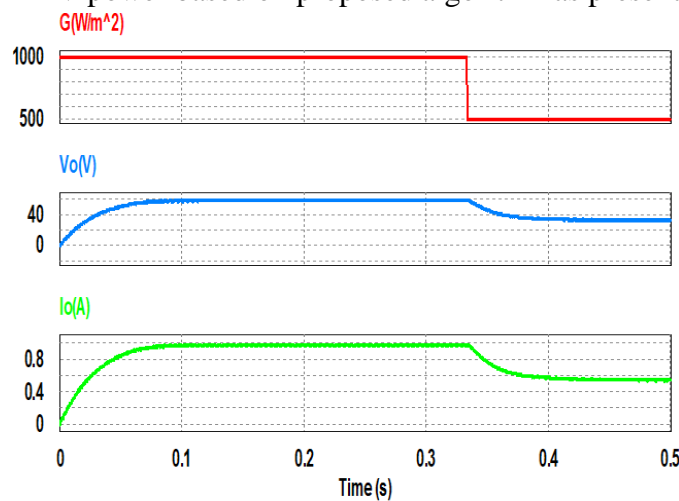


Fig. 11. Simulation results at rapid change of irradiance and constant temperature $T = 25^{\circ}\text{C}$. Top to bottom: irradiance, output voltage, output current.

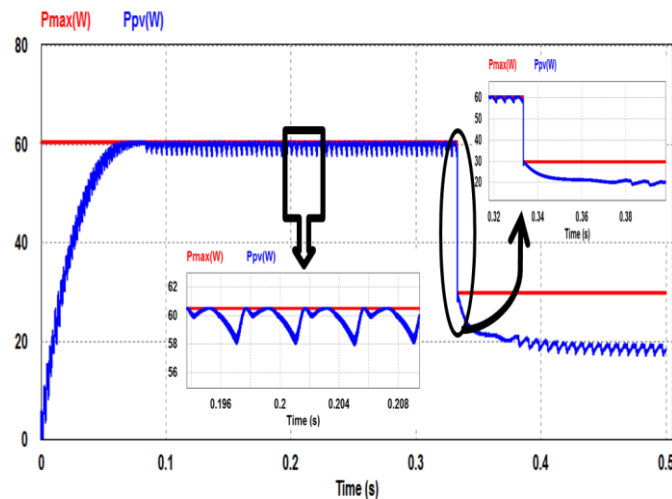


Fig. 12. Tracking the PV power according to ideal PV power in rapid change in irradiance level.

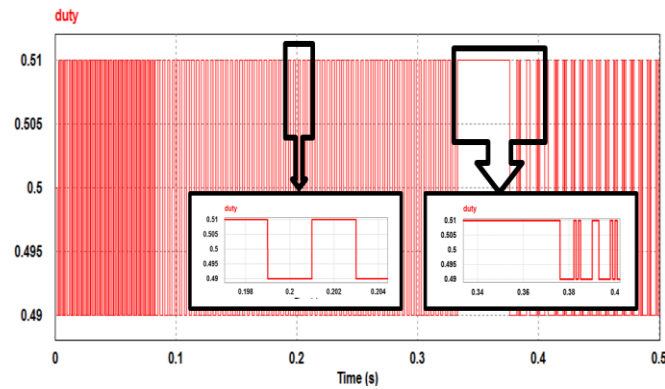


Fig. 13. Duty cycle of proposed MPP tracker under rapid change in irradiance level.

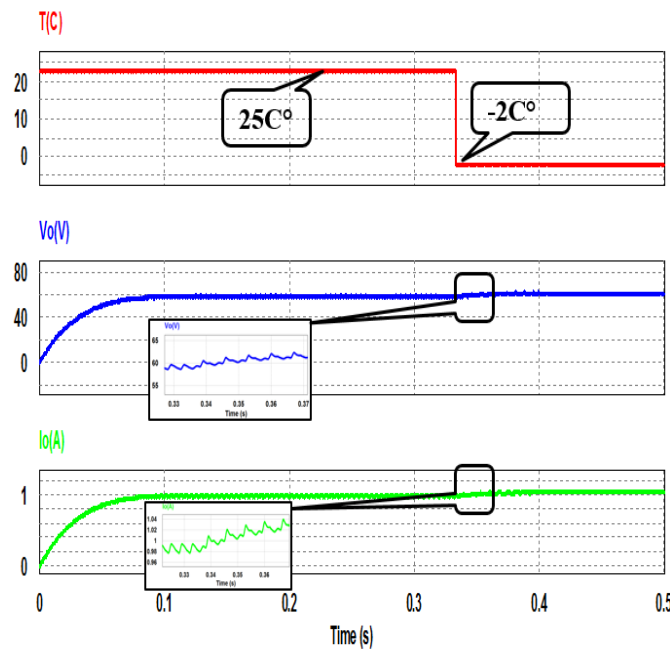


Fig. 14. Simulation results at rapid change of temperature and constant irradiance $G = 1000\text{W}/\text{m}^2$. Top to bottom: temperature, output voltage, output current.

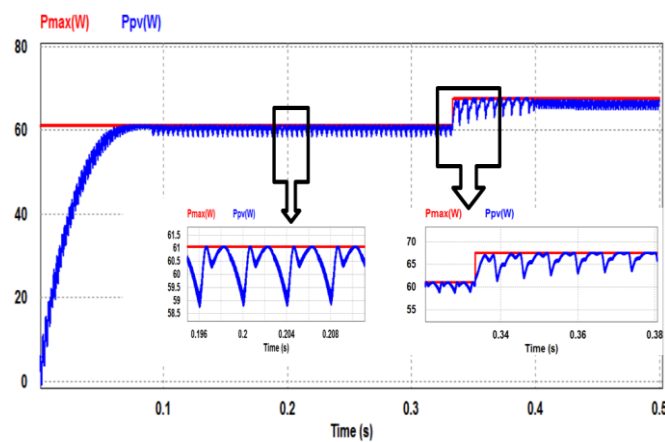


Fig. 15. Tracking the PV power according to ideal PV power in rapid change in temperature level.

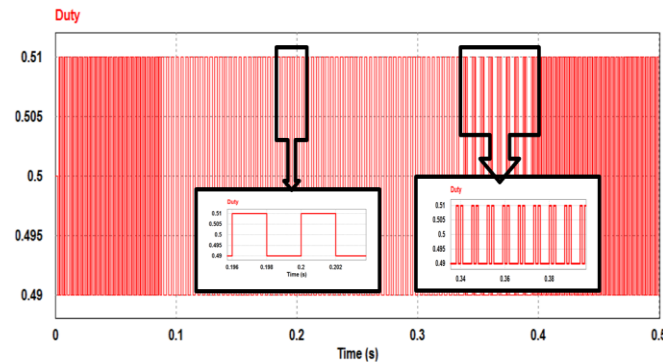


Fig.16. Duty cycle of proposed MPP tracker under rapid change in temperature level.

6 Conclusion

The outcome of this paper is to designed and simulated a low cost and simple MPP tracker. The proposed method has designed based on the perturbation of the PV power to get the optimal MPP at any weather condition. The flyback converter is analyzed using the mathematical equations to obtain the relationship of the input resistance that seen by the PV panel, load resistance, and duty cycle. As a result, by changing the duty, the equivalent input resistance has adjusted and then the MPP has been accomplished. The duty cycle is changed according to the perturbation of PV power. The proposed method is modeled and simulated in PSIM software and that algorithm is written directly using simple C-block code to build the MPP tracker. Finally, the proposed tracker is succeed by obtaining the MPP under rapid change of weather condition with small ripple resolution.

7 References

- [1] J. Zhao, X. Zhou, Y. Ma, and W. Liu: A Novel Maximum Power Point Tracking Strategy Based on Optimal Voltage Control for Photovoltaic Systems Under Variable Environmental Conditions, Elsevier publisher, Solar Energy, vol.122, Sep. 2015, pp. 640 – 649.
- [2] Salam J. Yqoob, A. A. Obed: Photovoltaic Flybck Micro-inverter with Power Decoupling Technique, Indonesian Journal of Electrical Engineering and Computer Science (IJEECS) vol.15, no.1, July 2019, pp. 9 –19.
- [3] A. S. Mahdi, A. K. Mahamad, S. Saon, T. Tuwoso, Hakkun Elmunsyah, and S. W. Mudjanarko: Maximum power point tracking using perturb and observe, fuzzy logic and ANFIS, Springer, SN Applied Sciences, Dec. 2019.
- [4] M. Janusz and M. Ostrowski: A low cost maximum power point tracker with the hybrid algorithm that uses temperature measurement, IEEE 8th International Conference on Renewable Energy Research and Applications (ICRERA), 2019.
- [4] S. Saravanan, and N. Ramesh Babu: Maximum power point tracking algorithms for photovoltaic system–A review, Renewable and Sustainable Energy Reviews, vol.57, 2016, pp. 192 –204.
- [5] K. Javed, H. Ashfaq, and R. Singh: A new simple MPPT algorithm to track MPP under partial shading for solar photovoltaic systems, International Journal of Green Energy, <https://doi.org/10.1080/15435075.2019.1686001>, Nov. 2019.
- [6] J. Prasanth Ram, T. Sudhakar Babu, and N. Rajasekar: A comprehensive review on solar PV maximum power point tracking techniques, Elsevier publisher, Renewable and Sustainable Energy Reviews vol.

- 67, Sep. 2017, pp.826 –847.
- [7] R. Shun-cheung Yeung, Henry Shu-hung Chung, Norman Chung-fai Tse, and Steve Tzu-hsiung Chuang: A global MPPT algorithm for existing PV system mitigating suboptimal operating conditions, Elsevier publisher, Solar Energy, vol.141, Jan.2017, pp. 145 –158.
- [8] S. Motahhir, A. El Ghzizal, S. Sebti, A. Derouich, and A. Ghzizal: Proposal and implementation of a novel perturb and observe algorithm using embedded software, IEEE 3rd International Renewable and Sustainable Energy Conference, Marrakech, Morocco, Dec 2015, pp.1 - 5,
- [9] A. Rozana, and Awang Jusoh: An enhanced P&O checking algorithm MPPT for high tracking efficiency of partially shaded PV module, Solar Energy, vol.163, 2018, pp. 570 –580.
- [10] M. Kaouane, B. Akkila, and A. Cheriti: Implementation of incremental-conductance MPPT algorithm in a photovoltaic conversion system based on DC-DC ZETA converter, IEEE 8th International Conference on Modelling, Identification and Control (ICMIC), 2016.
- [11] R. Faraji, H. Naji, A. Rouholamini, M. Chavoshian and R. Fadaeinedjad: FPGA-Based Real Time Incremental Conductance Maximum Power Point Tracking Controller for Photovoltaic Systems, IEEE, IET Power Electronics, vol. 7, no.5, 2014, pp. 1294–1304.
- [12] T. Esum, and P. Chapman: Comparison of Photovoltaic Array Maximum Power Point Tracking Techniques, IEEE Transactions on Energy Conversion, vol.22, no.2, June, 2007, pp. 439 –449.
- [13] N. Pellet, F. Giordano, M. Ibrahim Dar, G. Zakeeruddin, S. M., Maier, and M. Grätzel: Hill climbing hysteresis of perovskite-based solar cells: a maximum power point tracking investigation, Progress in Photovoltaics: Research and Applications, vol.25, no.11, 2017, pp.942–950.
- [14] M. Kermadi, and El Madjid Berkouk: Artificial intelligence-based maximum power point tracking controllers for Photovoltaic systems: Comparative study, Elsevier publisher, Renewable and Sustainable Energy Reviews, vol.69, Nov. 2017, pp.369–386.
- [15] S. Messalti, A. Harrage and A. Loukriz: A New Neural Networks MPPT Controller for PV Systems, IEEE 6th International Renewable Energy Congress (IREC), 2015, pp. 1–6.
- [16] Waleed I. Hameed, Ameer L. Saleh, Baha A. Sawadi, Yasir I. A. Al-Yasir, and Raed A. Abd-Alhameed: Maximum Power Point Tracking for Photovoltaic System by Using Fuzzy Neural Network, Inventions, Vol. 4, No.33, 2019, pp. 1–12.
- [17] D. Bawa and C. Patil: Fuzzy Control Based Solar Tracker Using Arduino Uno, International Journal of Engineering and Innovative Technology (IJEIT), vol. 2, no.12, June 2013, pp. 179–187.
- [18] H. Bellia, R. Youcef, and M. Fatima: A Detailed Modeling of Photovoltaic Module using MATLAB,” NRIAG Journal of Astronomy and Geophysics, vol. 3, no. 1, May, 2014, pp. 53–61.
- [19] Salam J. Yaqoob, and Adel A. Obed: Modeling, Simulation and Implementation of Photovoltaic Panel Model by Proteus Software Based on High Accuracy Two-diode Model, Journal of Techniques vol.1, no.1, Dec. 2019, pp.39–51.
- [20] C. Vimalarani and N. Kamaraj: Modeling and performance analysis of the solar photovoltaic cell model using Embedded MATLAB, Transactions of the Society for Modeling and Simulation International, 2015, pp. 1–16.
- [21] Adel M. Dakhil, Ahmed Raisan Hussein and Ameer L. Saleh, Transformer-less Single-phase Inverter Based on SPWM Technique for Standalone PV Application, Solid State Technology, Vol. 63, No. 3, 2020, pp. 4088–4101.
- [22] H. A.Sher, K. E. Addoweesh and K. Al-Haddad: Performance Enhancement of a Flyback Photovoltaic Inverter using Hybrid Maximum Power Point Tracking, IEEE, 1st Annual Conference in Industrial Electronics Society (IECON), Yokohama, Nov. (9-12), 2015, pp. 005369 – 005373.

- [23] Young-Ho Kim, Young-Hyok Ji, Jun-Gu Kim, Yong-Chae Jung, and Chung-Yuen Won: A New Control Strategy for Improving Weighted Efficiency in Photovoltaic AC Module-Type Interleaved Flyback Inverters, *IEEE Transactions on Power Electronics*, vol. 28, no. 6, June, 2013.
- [24] Y. Kim, J. Kim, Y. Ji, C. Won, and T. Lee: Flyback Inverter Using Voltage Sensor-less MPPT for AC Module Systems, *IEEE Power Electronics Conference (IPEC)*, Jun. 2010, pp.948–953.
- [25] M. E. Basoglu and B. Cakir: Comparisons of MPPT Performances of Isolated and Non-isolated DC-DC Converters by using A New Approach, Elsevier publisher, *Renewable and Sustainable Energy Reviews*, vol.60, Jan. 2016, pp.1100–1113.
- [26] Keng C. Wu “Switch-Mode Power Converters: Design and Analysis: Elsevier Academic Press, ISBN 0-12-088795-9, USA, 2006.
- [27] Ameer L. Saleh , Adel A. Obed , Zainab Abdullah Hassoun , Salam J. Yaqoob, “Modeling and Simulation of A Low Cost Perturb& Observe and Incremental Conductance MPPT Techniques In Proteus Software Based on Flyback Converter”, 3rd International Conference on Sustainable Engineering Techniques (ICSET 2020), IOP Conf. Series: Materials Science and Engineering 881, 2020, pp. 1-15.